

Development of Grip-type Master Hand “MeisterGRIP”

Katsunari Sato, Shuji Komeiji, Naoki Kawakami, and Susumu Tachi, *The University of Tokyo*

Abstract—We propose a novel grip-type master hand called MeisterGRIP that measures grip force in terms of a force vector distribution. This device is expected to allow intuitive robot manipulation using vision-based haptic-sensing technology. Furthermore, it can be used for general-purpose manipulation and is tolerant to individual differences in hand size and grasping posture. We constructed MeisterGRIP and evaluated the accuracy of the measured grip force. Furthermore, we constructed and exhibited a complete robot manipulation system using MeisterGRIP to demonstrate the possibility of using MeisterGRIP as a general-purpose master hand.

I. INTRODUCTION

TELEXISTENCE or telepresence is an advanced form of teleoperation that enables humans to remotely perform tasks with dexterity, providing the operator with the illusion of being actually present at the remote location [1]. This technology finds application not only in expert fields, but also in communication and entertainment for the general public. However, previous telexistence technologies were mainly developed for expert applications such as in the da Vinci surgical system [2]. Nevertheless, in the future, telexistence technology will be more common and will be considered a general-purpose technology. For example, it will allow us to shake hands with friends living in a different country or to climb a mountain—to actually touch the rocks and plants—while sitting in the living room.

To realize a telexistence system that can be used by a lay individual, we believe that a simple and universal control system employing a robotic hand (master hand) should be developed. The master hand is important when interacting with a remote environment because it allows the generation of realistic sensations. We believe that there are three requirements for the general-purpose master hand. First, it should be easy to use, i.e., it should function intuitively. Second, the system should be usable by a wide cross section of individuals. To be accepted by general households, anyone—men, women, and children—should be able to use the master hand easily. Finally, the system should enable robotic hands to grasp fragile objects gently.

A short survey of conventional master hand systems

available today reveals that few systems, if any, satisfy the abovementioned requirements. Master hand systems that allow another fully robotic hand to mimic the operator’s movements have been developed. These master hand systems measure the operator’s movements directly by using a wearable device [3] or indirectly by using optical or magnetic transducers [4] [5]; both methods enable intuitive and correct robot manipulation. However, both methods require the use of additional attachments to control the grasping force. Other types of master hands have been developed that use efferent neuronal signals such as myoelectric signals [6]. Because vision is superior to somatic sensation, even if their body does not actually move, operators will feel as though they themselves have moved, when they receive visual feedback that the robotic hand has moved. Therefore, this type of master hand also enables intuitive manipulation and can be rendered into a compact system. Furthermore, it allows the control of grasping force. However, myoelectric signals cannot be easily detected with high accuracy using such systems, which can also be troublesome to wear.

We believe that a master hand should be developed such that anyone can use it intuitively and easily. In addition, we aim to realize gentle grasping by enabling the control of grasping force. In order to satisfy these requirements, we have developed a novel master hand called “MeisterGRIP.” This device measures the operator’s grip force and uses this information to control the robotic hand (Figure 1.) For this purpose, the operator is simply required to grasp the device; therefore, the complexity of the setup is reduced, and there are fewer restrictions on the operator. Furthermore, by reflecting the grasping force of the operator directly in the robotic hand, intuitive manipulation is made possible. In this paper, we introduce MeisterGRIP and describe an evaluation of the accuracy of the measured grip force.

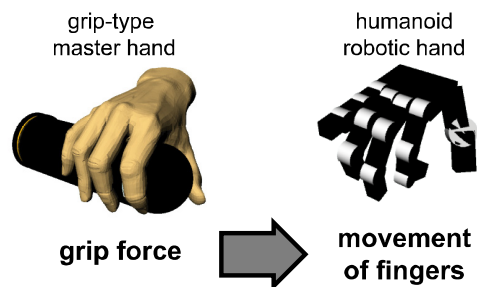


Fig. 1. Principle underlying grip-type master hand

Katsunari Sato, Shuji Komeiji, Naoki Kawakami, and Susumu Tachi are affiliated with the Graduate School of Information and Technology, The University of Tokyo, Japan; e-mail: (Katsunari_Sato, Shuji_Komeiji)@ipc.i.u-tokyo.ac.jp, (kawakami, tachi)@star.t.u-tokyo.ac.jp.

This work was supported by Grant-in-Aid for SCOPE and JSPS Fellows.

II. GRIP-TYPE MASTER HAND “MEISTERGRIP”

MeisterGRIP measures the operator’s grip force and uses it to control the robotic hand. In order to measure the grip force, we used the three-dimensional force vector distribution created by the act of grasping. Using the force vector distribution, we can relate the grip force to complicated finger movement. When an operator grasps our proposed device, the device recognizes the five fingers of the operator as five input positions on the basis of the force applied to the device by each finger. Then, the force vectors resolved to the three axes are measured at each input point and relayed to each finger of the robotic hand. The input points could be at any position on the device surface; this allows the operator to grasp the device at any position and in any posture. The individual differences among the hand sizes are also compensated by this feature. Furthermore, the grasping force of the robotic hand can be adjusted by controlling the robotic fingers by the force of operator’s fingers.

In order to measure the force vector distribution, we used our vision-based haptic-sensing technology [7]. The haptic sensor consists of a transparent elastic body with two layers of a marker matrix and a color camera. When a force is applied to the surface of the sensor, the markers move. The movement of the markers is captured by the camera. We determine the location of the center of the markers before and after the application of force. Therefore, we can record the movements of markers and calculate the applied force using equation (1).

$$f = (H^T H)^{-1} H^T u. \quad (1)$$

In this equation, u , f , and H denote the two-dimensional movement vectors of the red and green markers as captured by the camera, the three-dimensional force vector, and the conversion matrix, respectively. The elements of H are calculated by using elastic theory [8].

It should be noted that we make two assumptions to calculate the force vector field from the movements of the markers: (a) the sensor is assumed to be a semi-infinite elastic body; and (b) the deformation of the elastic body is assumed to be linear.

III. CONFIGURATION OF MEISTERGRIP

To measure grip force, the device should be easy to grasp and should be such that the thumb faces the other fingers while grasping. For this, we considered a grip-type (cylindrical) device to be most suitable and developed a cylindrical vision-based haptic sensor called MeisterGRIP.

Figure 2 shows the configuration of MeisterGRIP. We wrap an elastic body (resin replicating the properties of human skin: Hitohada gel, EXSEAL Inc.) around a transparent acrylic pipe. The surface of the elastic body is covered with black silicon rubber (KE-109, Shin-Etsu

Chemical Co.). Two layers of colored markers are also on the surface. The cylindrical body makes it difficult to capture the markers on camera. It would be difficult to place the cameras inside the cylindrical device because of their size. Further, if we use wide-angle cameras to track the markers, adjusting the focus becomes difficult. Therefore, we use hemispherical mirrors like those used in 360° panoramic cameras. Two cameras (Firefly MV, ViewPLUS Inc.) are attached at the two ends of the cylindrical body, and the hemispherical mirrors are attached at the center to track the markers effectively.

A fully constructed MeisterGRIP is shown in Figure 2. The device is designed to correspond to the hand of the average adult man: its length is 140 mm; diameter, 80 mm. An aluminum frame holds the elastic body, cameras, and mirrors in place. The diameter of the mirrors is 30 mm. Furthermore, to illuminate the red and green markers, we attach LED arrays to both sides of the cylindrical body. To capture the markers clearly, their diameters are set to 1.5 mm. Moreover, in order to prevent the overlapping of the red and green markers, they are separated by a distance of 4.0 mm. The red and green markers are placed at depths of 1.0 and 3.0 mm, respectively, from the surface of the device.

IV. CALCULATION OF GRIP FORCE

Because of the cylindrical shape of MeisterGRIP, we use different algorithms that are employed in conventional vision-based haptic sensors to calculate the force vector distribution. In this section, we introduce the algorithms used in MeisterGRIP for calculating the grip force.

A. Summary of Algorithm

The algorithm used to calculate the force vector distribution is shown in Figure 3. The algorithm consists of two separate steps: initialization and force calculation. During initialization, the initial position of the markers is captured. Then, finger positions used for grasping are identified. During force calculation, the force vector distribution at the finger positions is determined on the basis of marker movement. In both steps, the marker position should be captured and converted approximately.

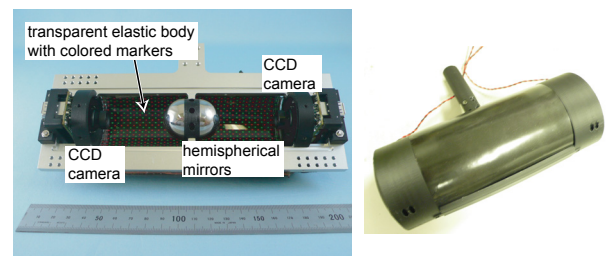


Fig. 2. Configuration of MeisterGRIP (right: profile, left: outer appearance)

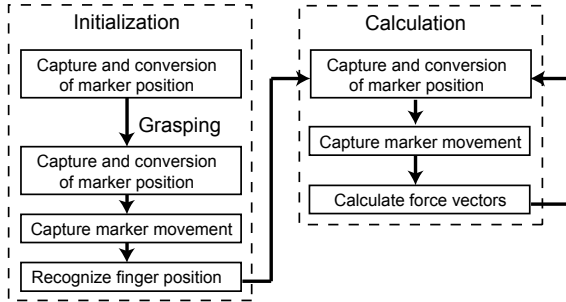


Fig. 3. Algorithm used to calculate force vectors

B. Capture and Conversion of Marker Position

Capture and approximate conversion of the marker position involves three steps: (a) the camera images should be captured and binarized; (b) the marker positions should be converted; and (c) the movement of the center of the markers should be calculated.

First, the captured color images are converted to grayscale images with red or green elements. Then, each grayscale image is binarized in order to capture the marker position. In the captured images, the luminance of the markers differs according to the marker position. Therefore, the image is binarized by using an adaptive thresholding algorithm. The adaptive thresholding algorithm binarize the image by changing the threshold dynamically over the image: the threshold of a pixel is the average luminance of the surrounding pixels.

Of the abovementioned initial steps, the second one is the most important for MeisterGRIP. The movement of the center of the markers should be calculated on a flat surface. However, the image recorded the reflection of the markers in the mirrors. Therefore, to the marker positions obtained from the images should be approximately converted to those that would be captured on a flat surface.

Figure 4 shows the image captured by the camera and the cross-sectional diagram of MeisterGRIP. We can calculate the approximate marker position (X, Y, Z) from the marker position in the captured image (u_i, v_i) using equation (2).

$$\begin{aligned} X &= Z\phi \\ Y &= y_i - Z / \tan \theta \\ Z &= R - D_R \end{aligned} \quad (2)$$

In equation (2), y_i , θ , and ϕ are calculated from u_i and v_i using equation (3).

$$\begin{aligned} y_i &= y_m + z_m / \tan \theta \\ y_m &= \sqrt{(u_i - u_c)^2 + (v_i - v_c)^2} \\ z_m &= \sqrt{r_m^2 - y_m^2} \\ \theta &= \alpha + 2\beta \\ \alpha &= \arctan(z_m / y_m) \\ \beta &= \arctan(z_m / (l - y_m)) \\ \phi &= \arctan(v_i / u_i) \end{aligned} \quad (3)$$

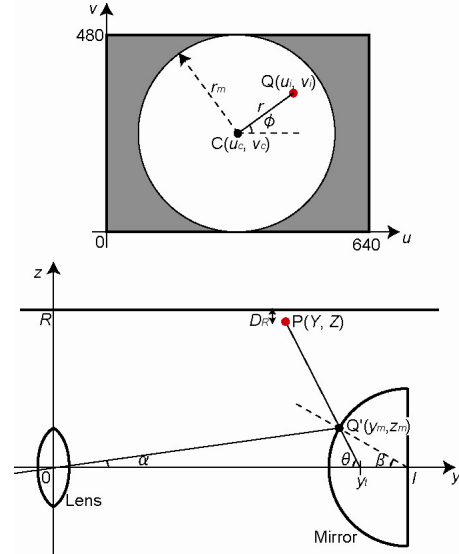


Fig. 4. Captured image and cross-sectional diagram used for determining the marker position. $Q(u_i, v_i)$ denotes the marker position in the captured image; $C(u_c, v_c)$, the center of the mirror; r_m , the radius of the mirror; $P(X, Y, Z)$, the approximated marker position; R , the radius of MeisterGRIP; D_R , the depth of the marker from the surface; and l , the distance between the mirror and camera lens.

Using these equations, we can convert the marker positions obtained from the captured image to those that would have been obtained on a flat surface. It should be noted that we use two cameras to capture the marker positions. Therefore, we converted and combined the marker positions to a flat surface.

Using the approximated marker positions, we calculate marker movement. To calculate the movement, we calculate the difference between the current and the initial positions of marker. The marker position is calculated from its center of the gravity.

C. Recognition of Finger Position

Recognition of the finger position is also important for MeisterGRIP. The system supports all hand sizes, grasping postures, and positions. Finger position is recognized when the sensor is first grasped and remains unchanged even when the operator releases MeisterGRIP.

To recognize the finger position when an operator grasps MeisterGRIP, we use the movement of the center of the markers. When MeisterGRIP is grasped, the markers around the five fingers move more than the other markers. Therefore, we can estimate the finger position from the center of gravity of the absolute value of the movement of the markers.

D. Calculation of Grip Force

We calculate the grip force at each input point from the force vector distribution. In conventional vision-based haptic sensors, the force vector distribution over the whole surface of the sensor is calculated from all the marker

movements. In contrast, in MeisterGRIP, because we approximate the camera image, using all marker movements can introduce errors in the calculation. Furthermore, calculating the force vector distribution over the whole surface can prove to be wasteful. We believe that it is enough to calculate the force vector distribution over the contact field between the fingertips and the surface of the device.

Therefore, in MeisterGRIP, we calculate the force vectors at nine (three times three) calculation points around the input points. The vision-based haptic sensor calculates the most accurate force vector corresponding to the force applied at the measurement point. Therefore, calculating the force vector at the input points improves the accuracy of the measurement. The distance between the calculation points is 5.0 mm. The markers used in this calculation are within the 15.0 mm from the input points. After the calculation of the force vectors, we sum all the calculated force vectors. We use this value as the grip force of each finger (Figure 5). In the calculation loop, this algorithm consumes only 30 msec on a desktop computer (2.8 GHz, Intel Pentium D processor).

V. EVALUATION

In teleexistence, the master hand should be able to remotely perform grasping as if it were an operator's hand. Therefore, MeisterGRIP should be capable of measuring the grip force of each finger correctly and independently. We evaluated the accuracy of the measurement of three-dimensional grip force at each finger and whether the forces are independent of each other.

A. Experimental Setup

The experiment consisted of two parts; evaluation of accuracy and verification of the independence of forces. In both the experiments, we applied an arbitrary force to the surface of MeisterGRIP by using a six-axis force sensor (BL AUTOTEC Inc.). Furthermore, we recorded the calculated force vector and the output of the six-axis force sensor in order to compare them. The experimental setup is shown in Figure 6. We used XYZ-stage (CHUO PRECISION INDUSTRIAL Co.) to apply the force at the end of the six-axis force sensor. The diameter of the contact surface of the six-axis force sensor was 10 mm.

In MeisterGRIP, to calculate the grip force, markers reflected by the mirrors were captured. Then, the captured marker positions were approximated to those that would have been obtained on a flat surface. This approximation might cause calculation error in the y and z directions. This error might be particularly prominent at the center and edge of the device. Therefore, we evaluated the grip force at three different measurement points A, B, and C on the surface (Figure 6). A, B, and C were at 70 mm, 45 mm, and 20 mm, respectively, from one end of the cylindrical body.

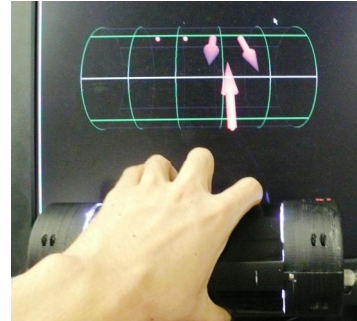


Fig. 5. Measured grip force. Green lines and red arrows represent the cylindrical shape of the device and the grip forces, respectively.

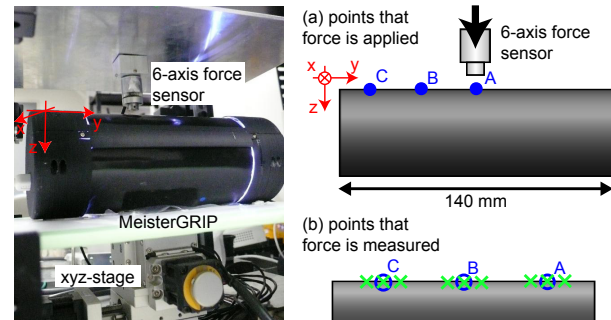


Fig. 6. Experimental setup. Blue dots and green crosses represent points where the force is applied and is measured, respectively.

In order to evaluate the accuracy of the grip force, we evaluated the linearity of the grip force in the three axes. We applied force at the input position while changing its magnitude and direction. We applied force at three points and evaluated the accuracy of the grip force. Prior to the evaluation, we normalized all the measured force by the average measured force at point B for calibration purposes. In order to verify the independence of the forces, we applied a z-directional force to a point and measured the force vector at three points: the point at which the force is applied and around it. Then, we evaluated the influence of the applied force on points where the force is not applied.

B. Accuracy of Measured Grip Force

We applied the x- and y-directional forces in the range 0 to 500 gf at 100 gf intervals along with a 1000-gf z-directional force. Then, we applied a z-directional force in the range 0 to 1000 gf at 100 gf intervals. In each trial, we measured the force five times and evaluated the average of the measurements.

Figure 7, 8, and 9 show the linearity of the measured force along each axis. In these figures, the horizontal and vertical axes represent the applied force and measured force normalized by the maximum value, respectively. The blue argyles, the green squares, and the red triangles represent the average of the measured force when we applied force to the point A, B, and C, respectively. The bars represent the standard error.

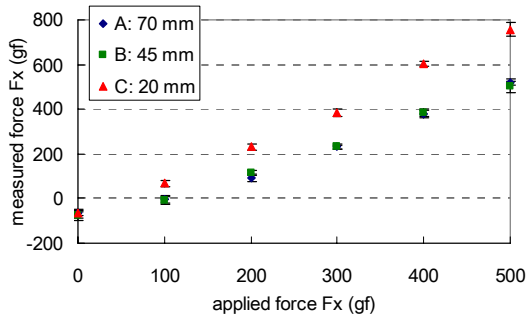


Fig. 7. Linearity of measured force F_x .

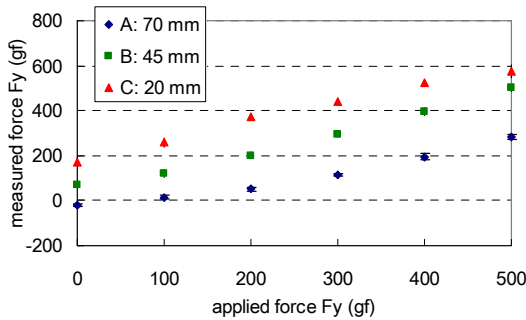


Fig. 8. Linearity of measured force F_y .

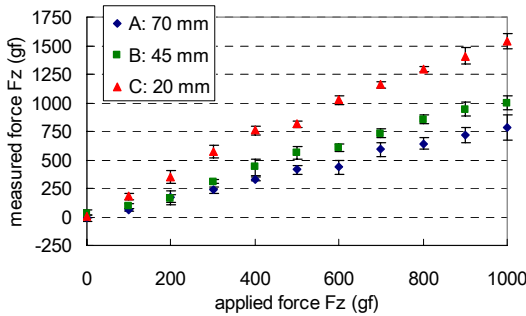


Fig. 9. Linearity of measured force F_z .

The results show that the measured grip force is linear in all directions. The resolved forces in the x-y direction and the z-direction are approximately 30 gf and about 70 gf, respectively. The magnitude of the force measured at different points differs.

C. Independence of Force Vectors

We chose three measurement points in the y-direction and applied 300-, 600-, and 900-gf z-directional forces at these points. The distance between the applied force and the closest measurement point was in the range 5.0 to 15.0 mm at 2.5 mm interval. We normalized the measured force by using the measured force at force applied point.

Figure 10 shows the independence of the measured force at each point. In the figure, the horizontal and vertical axes represent the distance of the nearest measurement point from

the applied force and the measured force normalized using the maximum value, respectively. The blue argyles, green squares, and red triangles represent the average of the measured force at point A, B, and C, respectively. The bars represent the standard error.

When the distance of the nearest measurement point from the applied force is more than 10.0 mm, the normalized measured force is less than 40 % of that obtained at the applied force. This suggests that the grip force can be independently measured when the input points are separated by more than 10.0 mm from the applied force.

D. Discussion

In the experiment investigating the accuracy of the measured grip force, the linearity of MeisterGRIP was confirmed. Furthermore, the resolved forces were considered sufficient for the analog control of robotic the hand to grasp an object. However, the magnitude of the measured force differs among different measurement points: the measured force at A is smaller than that at B, and the measured force at C is larger than that at B. It is possible that the approximation of marker positions caused some errors. In MeisterGRIP, we capture the reflected marker image in hemispherical mirrors. Thus, the converted marker movements in the y-direction were not accurate. Therefore, the conversion matrix in equation (1) should be modified so as to reduce the influence of marker movements on the calculation.

The results of our experiments also revealed that the force vectors are independent even when the distance between the two input points is 10.0 mm, which is corresponds to the size of the fingertip of an average adult man. Furthermore, the independence of the force vectors might be improved by increasing the density of markers because the independence of the force vectors is influenced by the spatial resolution of the measured force vector distribution. Therefore, we can conclude that MeisterGRIP is capable of measuring the grip force independently regardless of the operator's size/posture.

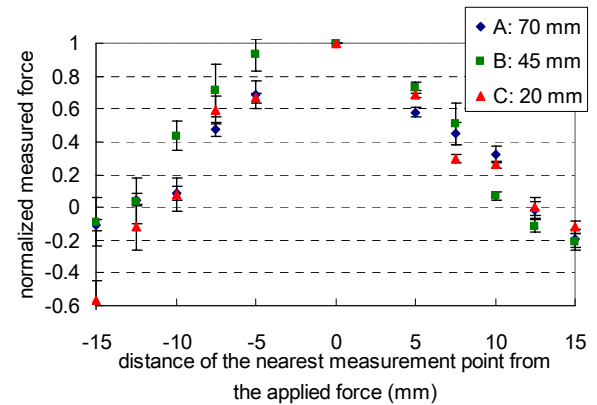


Fig. 10. Independence of grip force.

VI. ROBOTIC HAND CONTROL

Using MeisterGRIP, we constructed a manipulation system comprising robotic hands and arms (cockpit). The configuration of the cockpit is shown in Figure 11. We used electrically actuated humanoid robotic hands and air-actuated seven degree of freedom (DOF) robotic arms. We used the grip force measured by MeisterGRIP to control the five-fingered robotic hands. To control the robotic hands, the measured force information was used to calculate the velocity of movement of the robotic fingers. Therefore, the stronger the grasps of the operator on MeisterGRIP, the faster is the movement of the robotic fingers. Each robotic finger has one DOF, so we used only the magnitude of the force vectors to control each finger. We attached MeisterGRIP to the master arms, which measure the movement of MeisterGRIP (DOF: 2). When the operator grasps MeisterGRIP and moves his/her hand, the potentiometer attached to the master arm measures the hand movement. This information is relayed to the robotic hand, which moves accordingly from right to left or up and down. Furthermore, the torque applied by the operator is measured by MeisterGRIP and mimicked by the robotic hands through yaw-axis rotation. To control the position and posture of the robotic hands, we control the robotic arm. This is accomplished by using a PID algorithm.

We exhibited the constructed cockpit at SIGGRAPH 2008 New Tech Demo [9] and interactive-Tokyo 2008 [10]. Through these exhibitions, more than one thousand people experienced the ability to control robotic hands and arms using MeisterGRIP. At the exhibitions, visitors were asked to grasp and pick up balloon animals, and about half the volunteers, regardless of sex and hand size, could accomplish this task within a few minutes. Furthermore, some of these volunteers commented on the ease of robotic control allowed by MeisterGRIP. Therefore, we can consider MeisterGRIP to be a general-purpose master hand.

However, some of the volunteers had suggested that receiving a feedback indicating contact with the object could assist in accomplishing the task of manipulating the object more effectively. In MeisterGRIP, operators always receive a reactive force when grasping the device. Thus, operators can feel force feedback and grasp an object stably. However, they cannot perceive the surface of the object, or the sensation of touching with their fingers. Therefore, MeisterGRIP should be equipped with a tactile display using vibration or electro-stimulus. Attaching an electrotactile display [11] to the MeisterGRIP might assist in realizing touch feedback.

VII. CONCLUSIONS AND FUTURE WORK

We constructed a novel grip-type master hand called MeisterGRIP. We evaluated the accuracy of the measured grip force and constructed a robot manipulation system.

MeisterGRIP was found to allow instinctive and dexterous robot manipulation on the basis of vision-based haptic-sensing technology. Furthermore, it allows universal manipulation, i.e., it compensates differences in the hand sizes and the grasping postures of the operators.

In the future, to improve the accuracy of the measured grip force, we intend to improve the conversion matrix of the equation (1). This could reduce the error in the approximation of the captured image. Furthermore, we intend to incorporate electrotactile feedback into MeisterGRIP to obtain a general-purpose master hand.

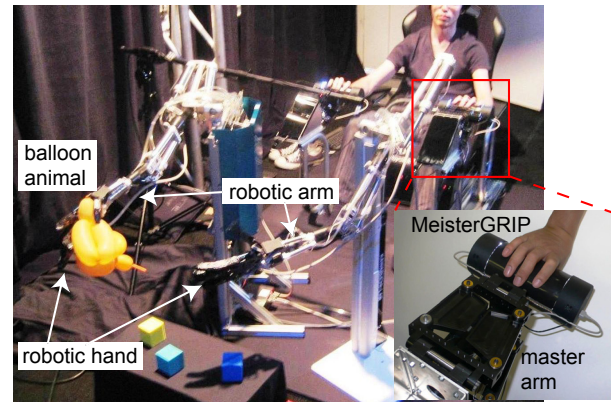


Fig. 11. System controlling robotic hands and arms by using MeisterGRIP.

REFERENCES

- [1] S. Tachi and K. Yasuda, "Evaluation Experiments of a Telexistence Manipulation System," *Presence*, Vol. 3, No.1, pp. 35–44, 1994
- [2] Intuitive Surgical Inc. da Vinci.
- [3] Immersion Technology Inc. Cybergrasp. <http://www.immersion.com/index.php>.
- [4] K.Hoshino and T.Tanimoto: "Real time search for similar hand images from database for robotic hand control," *IEICE Transactions on Fundamentals of Electronics, Communications and Computer Sciences*, E88-A, 10, 2005, pp.2514–2520.
- [5] K.Hoshino: "Interpolation and extrapolation of repeated motions obtained with magnetic motion capture," *IEICE Transactions on Fundamentals of Electronics, Communications and Computer Sciences*, E87-A, 9, 2004, pp.2401–2407.
- [6] M. Yoshikawa, T. Tsujimura, M. Mikawa, and K. Tanaka : "Human-machine Interface Using EMG Signals for Robot Hand Control," *The Society of Instrument and Control Engineers (SICE) Annual Conference 2005 in Okayama: Proceedings*, 2005, pp.2853–2858.
- [7] K. Kamiyama, H. Kajimoto, N. Kawakami, and S. Tachi, "Evaluation of a Vision-based Tactile Sensor," in *Proceedings of International Conference on Robotics and Automation 2004*, Vol. 2, 2004, pp. 1542–1547.
- [8] L. D. Landau and E.M.Lifshitz, "Theory of Elasticity," *ButterworthHeinemann*, 1985.
- [9] S. Komeiji, K. Sato, K. Minamizawa, H. Nii, N. Kawakami, and S. Tachi, "MeisterGRIP: cylindrical interface for intuitional robot manipulation," *SIGGRAPH Posters and New Tech Demo*, 2008.
- [10] S. Komeiji, K. Sato, M. Tazono, K. Minamizawa, H. Nii, N. Kawakami, and S. Tachi, "MeisterGRIP: cylindrical interface for intuitional robot operation," *interactive-Tokyo 2008*, 2008.
- [11] K. Sato, H. Kajimoto, N. Kawakami, and S. Tachi, "Electrotactile Display for Integration with Kinesthetic Display," in *Proceedings RO-MAN 2007*, 2007, pp.3–8.